JOURNAL OF MATERIALS SCIENCE 33 (1998) 707–712

The contributions of microstructural characteristics and residual stress distribution to mechanical properties of AlN/W composite system

YOUNG-HOON YUN*, SUNG-CHURL CHOI
Department of Inorganic Materials Engineering, Hanyang University 17, Hangdang, Sungdong, Seoul, South Korea

AlN–W composites were fabricated by pressureless sintering. The residual stress and mechanical properties were investigated for AlN–W composites with different tungsten contents. The fracture strength decreased and the fracture toughness increased with increase of the tungsten phase from 5 vol% to 20 vol%. It was thought that the decrease of strength would be due to the effects of relative density and the grain boundary phases. The crack tortuosity of indented specimens was gradually marked as a function of secondary phase content. In the residual stress measurement, the matrix phase of composites exhibited compressive stress distribution, which was increased with the addition of tungsten. This tendency was consistent with the results predicted by the thermoelastic stress model. From the results of the crack propagation path and the development of fracture toughness, it was thought that the residual compressive stress of matrix phase must have contributed to the development of crack propagation resistance. © *1998 Chapman & Hall*

1. Introduction

A ceramic–matrix composite is an important material in high-technology industries, because of its thermal and mechanical properties. The mechanical properties of ceramic–metal composites have been studied from the several standpoints, such as the observation of microstructural morphology, the theoretical calculation of thermal stress, and the residual stress measurement. Also, it has been well known that the microstructural features, especially the characteristics of ceramic–metal interface and the residual stress distribution of matrix phase, are critical in determining the fracture behaviour of composites [1, 2]. However, it is difficult to understand the effect of secondary phase on fracture behaviour by observing the microstructural morphology. The influence of residual stress has been investigated by some researchers [3, 4]; Michalske and Hellmann reported that toughness increases linearly with the increment of the residual compressive stress in matrix phase [2].

The purpose of present study is to investigate the effects of secondary phase on mechanical properties from observing the microstructure, the indentation-induced crack path, and measuring the residual stress distribution using the X-ray stress measurement method [5]. Also, the residual stress distribution of composites was predicted by thermoelastic stress model [6].

2. Experimental procedure

2.1. Preparation of specimens

In this work, AlN-powder (F-grade, mean particle size 1 μm, Tokuyama Soda., Japan) and tungsten- powder (KM-3, particle size distribution 0.3–0.7 μm, Korea Tungsten, South Korea) were used. Fig. 1 shows the experimental procedure. Table I shows the characteristics of AlN and tungsten material. For homogeneous dispersion, AlN and tungsten powder were mixed by the ultrasonic homogenizer (Model US-300T, Nissen, Japan) in isopropyl alcohol. The slurry was mixed with ZrO_2 ball in isopropyl alcohol for 24 h. In the drying process of the slurries, heating and mixing was simultaneously done using a hot plate. Monolithic AlN and AlN–5, 10, 15, 20 vol% W composites were prepared, the specimens were sintered for 2 h at 1900 °C under nitrogen atmosphere in a graphite furnace.

2.2. Characterization of AlN–W composites

The relative densities of sintered specimens were measured by Archimedes' method in toluene. A four-point bending strength test was carried out by UTM (AGS-500D, Shimazu Co, Japan) under the conditions of: cross-head speed of 0.5 mm min^{-1}, upper span of 10 mm, and lower span of 20 mm, and the fractured specimens were observed by scanning electron microscopy (SEM) (Model JSM-5200, Jeol, Japan). Also, fracture toughness was tested with a Vicker's microhardness tester (Torsee, Type: DVKH-1, Tokyo testing machine MFG Co., Ltd, Japan) with the conditions of load of 5 kg-f, duration of 15 s, loading speed of 70 μm s^{-1}. The ICL (indented/crack length) method was used to calculate toughness.

Crystal phases for monolithic AlN and AlN–W composites were characterized by X-ray diffraction analysis (40 kV, 30 mA) with Ni-filtered Cu$K\alpha$-radiation.

2.3. Measurement of residual stress by X-ray diffraction

It is possible to measure the residual stress in materials by X-ray diffraction and neutron diffraction. In present study, the $\sin^2\psi$ methods using an X-ray beam was used. As shown in the schematic illustration of Fig. 2, the stress measurement was carried out for five tilts ($\psi = 0$, 10, 20, 30 and 40°) at the optional direction (S_ϕ, S_1, S_2, S_3). At first, the original plane spacing (d_0) of a green specimen was measured. A green specimen was prepared by drying the slurry which had been mixed with isopropyl alcohol. The measurement of residual stress was executed by an X-ray goniometer system, which is composed of residual stress analyser and stress calculation program; the measurement conditions were as follows: 40 kV, 30 mA, step interval 0.02°, fixed times 30–70 s, step mode, CrK_α radiation. The (1 1 2) crystalline plane of AlN was chosen for stress measurement, and the shape of the detected peak is shown in Fig. 3. In the case of tungsten, the (2 1 1) plane was chosen. The variations of crystalline plane spacing were determined by measuring the peak shifts of diffracted plane. Then, residual stress was calculated by applying the elastic modulus and Poisson's ratio to spacing variations [5].

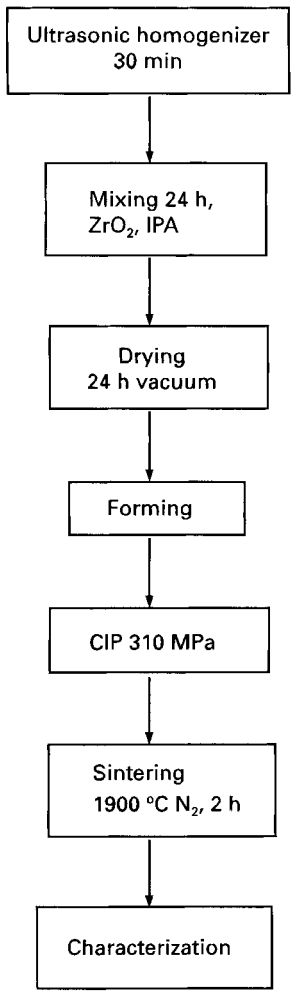

Figure 1 Flow chart of experimental procedure of monolith and composites.

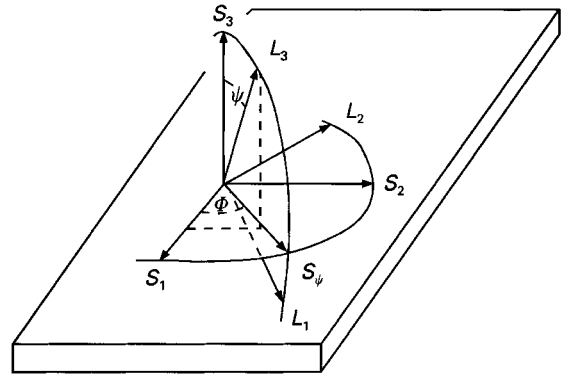

Figure 2 Schematic illustration of residual stress measurement.

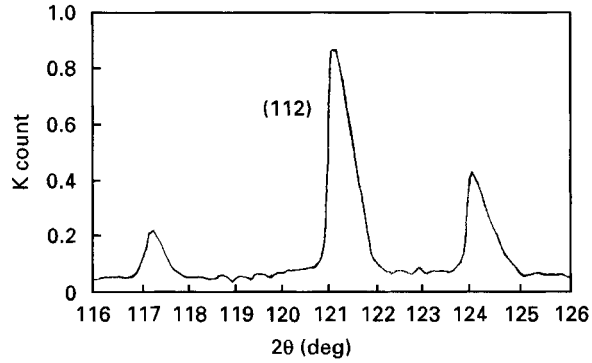

Figure 3 Diffraction pattern of (1 1 2) plane for AlN.

TABLE I Properties of AlN and tungsten

Properties / Material	Density ($g\,cm^{-3}$)	Thermal expansion coefficient ($\times 10^{-6}\,°C^{-1}$)	Fracture toughness ($MPa\,m^{1/2}$)	Elastic modulus (GPa)	Poisson's ratio	Melting point (°C)	Thermal conductivity ($W\,mK^{-1}$)
		5.9 (20–1520 °C)					
Aluminium nitride	3.26	*a*-axis: 5.3 *c*-axis: 4.2 (20 ~ 800 °C)	2 ~ 3	300 ~ 310	0.25	2300 (sublimation)	100 ~ 200
Tungsten	19.32	5.1 (27 ~ 1300 °C)	–	350	0.28	3410	140

From [7, 8].

3. Results and Discussion

3.1. Relative density and microstructure

Fig. 4 shows the relative densities of monolithic AlN and AlN–W composites. The relative density of monolithic AlN was about 90%, whereas, under the same sintering conditions, AlN–5 vol % W composite showed a relative density of nearly 99%. When the volume fraction of secondary phase was in the range of 10–20%, the relative density of composites decreased gradually.

The densification of composites was thought to be as follows. In general, it has been well known that the AlN particle surface is covered with the amorphous oxide phase [9], and also the tungsten particle will have tungsten oxide phases. Therefore, in the sintering process, the AlOOH phase [9] or the oxide phase on the AlN particle will create the liquid phase from the reaction with the tungsten oxide phases. Such a reaction could be predicted from the Al_2O_3–WO_3 phase diagram [10]. These liquid phases of grain boundary would have induced the rearrangement of particles [11–13], although, the solution–reprecipitation procedure through mass transfer between matrix grains which induces the densification of microstructure would be suppressed by the secondary phase and grain boundary phase. Fig. 5 indicates the grain growth of monolithic AlN, and it was presumed to be the result of a solution–reprecipitation process. On the other hand, in case of composites, the grain size of AlN matrix was diminished with the addition of secondary phase.

In the XRD patterns of Fig. 6, AlON phase and tungsten oxides ($WO_{2.9}$, $WO_{2.83}$, $WO_{2.7}$, WO_2) were identified; the solid solution phase of $Al_2(WO_4)_3$ was also detected.

3.2. Residual stress distribution of AlN–W composites

It is well known that residual stress plays an important role in the fracture behaviour of composites [3, 14]. However, mechanical properties have been investigated mainly by observing the microstructure for the difficulty of residual stress measurement. Generally, the residual stress of composites is caused by the difference between thermal expansion coefficient of matrix and that of secondary phase [14], and the elastic modulus will determine the extent of residual stress of each phase. In present study, the residual srtress of AlN–W composites was calculated by the thermoelastic stress model [6]. This model is derived

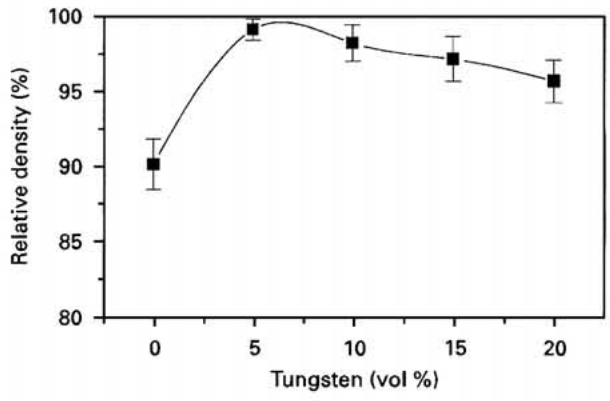

Figure 4 Relative density of monolithic AlN and AlN–W composites.

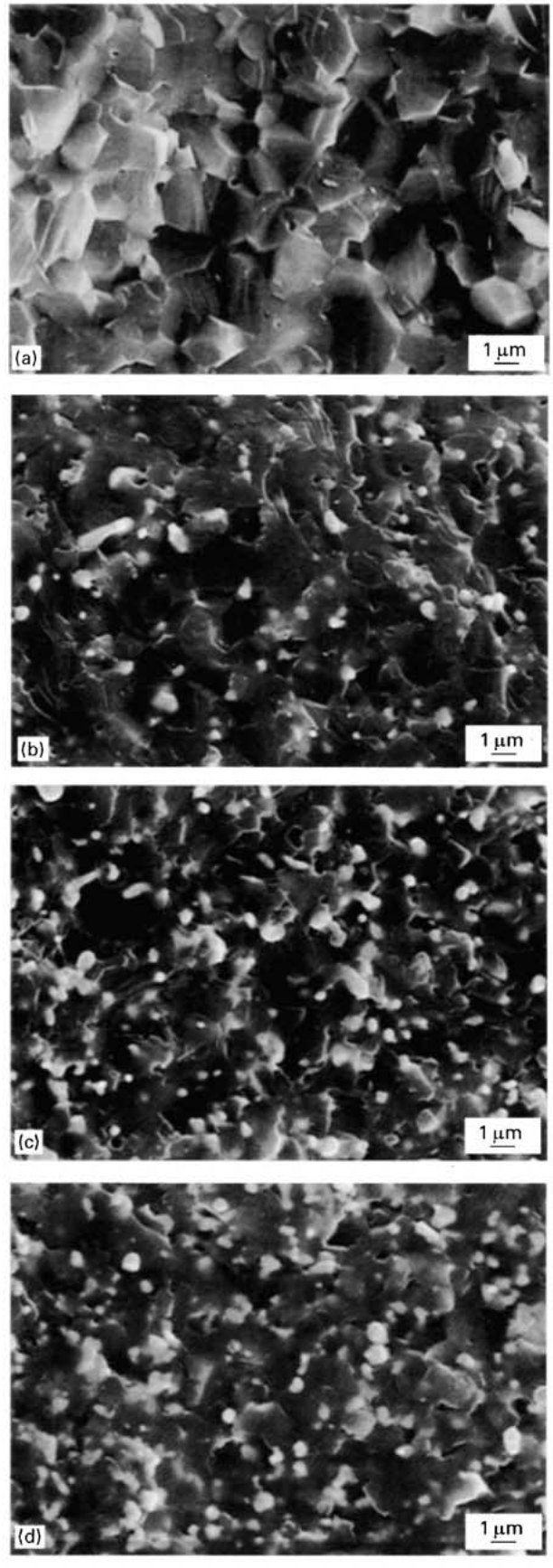

Figure 5 Microstructure of monolithic AlN and AlN–W composites. (a) AlN (b) AlN-5 vol% W (c) AlN-10 vol% W (d) AlN-15 vol% W (e) AlN-20 vol% W.

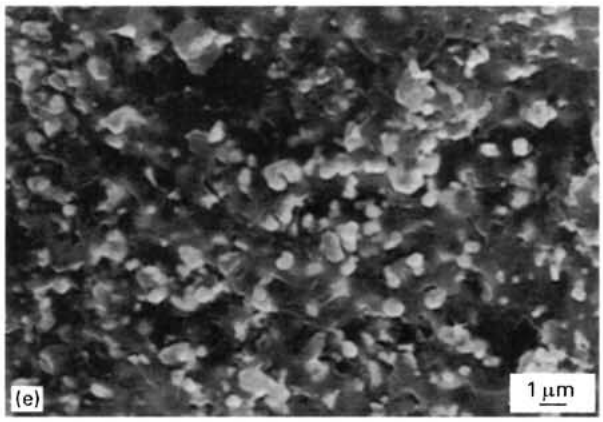

Figure 5 (Continued).

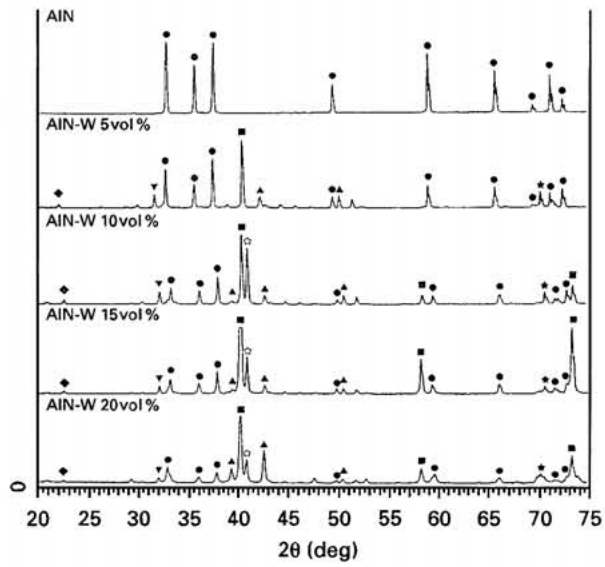

Figure 6 XRD patterns of monolithic AlN and AlN–W composites. (●) AlN; (♦) $WO_{2.7,2.9}$; (▼) AlON; (▲) $Al_2(WO_4)_3$; (☆) $WO_{2.83}$; (■) W; (★) WO_2.

from the matrix phase including the secondary phase under no applied stress. As shown in Equation 1, this calculation was executed for the secondary phase of a sphere $(R/r) = 1$, as in Fig. 7.

$$-\sigma_{rr} = 2\sigma_{\theta-\theta} = (\alpha_m - \alpha_p)\Delta T\left[\frac{1+\nu_m}{2E_m} + \frac{1+2\nu_p}{E_p}\right]^{-1}(R/r)^3 = P(R/r)^3 \quad (1)$$

where α_m and α_p are thermal expansion coefficients of matrix and secondary phase respectively, T is temperature, ν_m and ν_p are Poisson ratio of matrix and secondary phase respectively, E_m and E_p are elastic moduli of matrix and secondary phase respectively, R is radius of particles, r is distance from centre of particles and P is uniform pressure.

Table II shows the calculated stress of matrix of composites. In matrix phase, the radial stress component (σ_{rr}), having a compressive value, and the tangential stress component ($\sigma_{\theta\theta}$), having a tensile value, will be distributed during sintering process. Also, it could

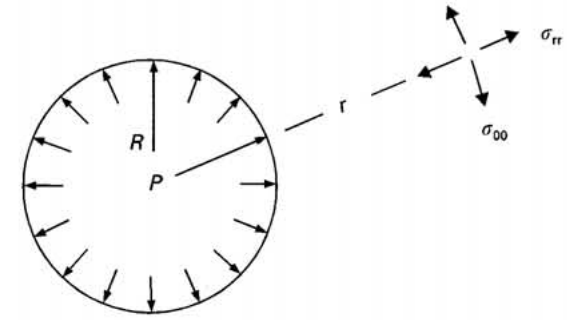

Figure 7 Residual stress field of spherical particle in infinite matrix.

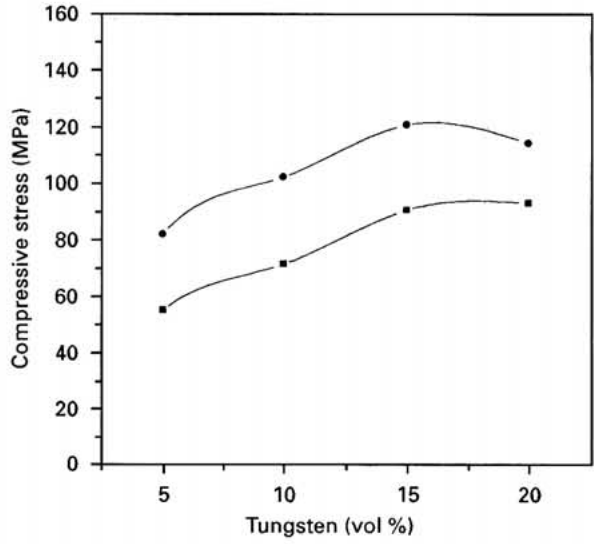

Figure 8 Residual stress distribution of AlN–W composites. (●) Maximum and (■) minimum stress values.

TABLE II Calculated stress for composites by thermoelastic stress model

Tungsten (vol %)	Calculated stress (MPa)
5	−20
10	−40
15	−60
20	−80

be supposed that residual stress field of the matrix phase would not be relaxed during the cooling process because of the strong covalent bonding of AlN. The results of stress measurement are shown in Fig. 8. The matrix phase showed the compressive stress field, which was augmented with the increase of secondary phase. Also, the residual tensile stress of secondary phase was identified by the same method. The results of stress measurement showed a similar tendency to that of the thermoelastic stress model. The compressive stress pattern of matrix in AlN–W composite is caused by the mismatch of thermal expansion coefficients and elastic modulus.

The calculated value and the measured value showed deviation, as shown in Fig. 8 and Table II. For the discrepancy between measurement and calculation and theoretical predictions, several considerations

have been suggested previously. In the formation of residual stress, the interaction of matrix and secondary phase is important, but subsidiary factors work upon the distribution of residual stress. The effects of these factors are appreciable in many cases. For example, these factors are: the cooling rate during sintering process, the size effect of matrix grain and secondary phase, the anisotropy of crystal structure, and the presence of other phases (grain boundary phases), etc. Thus, in stress measurement by X-ray method, the measured strains of the surface layer are converted into stresses using various assumptions as to the stress state and the anisotropy (preferred orientation). Also, the measured value is the average value over the surface depth, and the surface effect is included in the stress value. However, this technique is able to provide the approximate tendency of residual stress distribution, and the measured value does have significant meaning. Thus, the deviation of calculated value and measured value was inferred to be caused by the thermal expansion anisotropy of matrix and the interface phase (grain boundary).

3.3. Fracture strength and fracture toughness of composites

Fig. 9 shows the flexural strength of monolithic AlN and AlN–W composites. Despite the decrease of grain size, the flexural strength of AlN–W composites was decreased with the increase in tungsten content. This result would be due to the decrease of relative density with increasing the secondary phase content, and the presence of grain boundary phase [15,16]. In the observation of the stress–strain curve, the monolithic AlN showed typical linear behaviour because of the fast fracture behaviour, but the composites showed

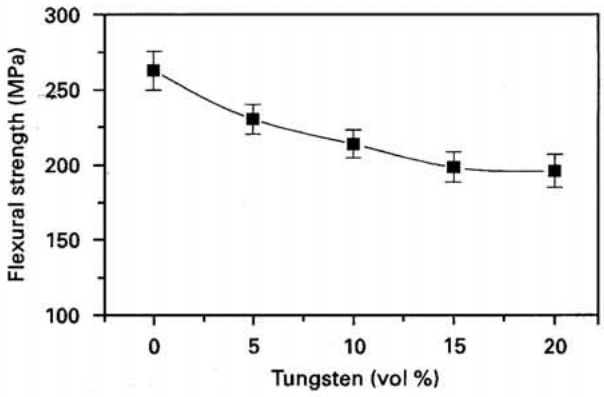

Figure 9 Flexural strength of monolithic AlN and AlN–W composites.

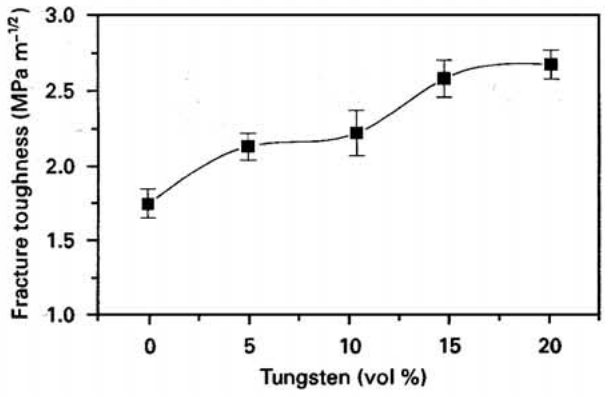

Figure 10 Fracture toughness of monolithic AlN and AlN–W composites.

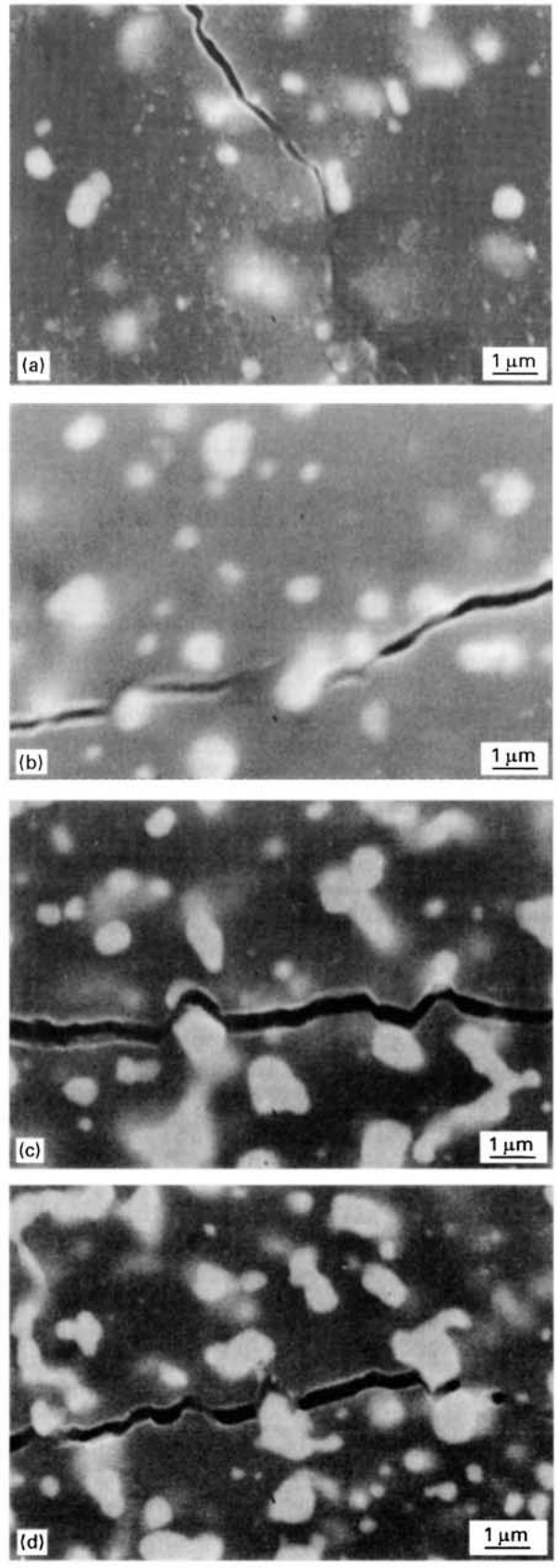

Figure 11 SEM micrographs of indented AlN–W composites. (a) AlN-5 vol% W (b) AlN-10 vol% W (c) AlN-15 vol% W (d) AlN-20 vol% W.

non-linear behaviour around the fracture stress. From the viewpoint of the microstructure, this phenomenon would be caused by the secondary phase, the grain boundary phase, and the variation of relative density. The stiffness variation around fracture stress would have caused the decrease in flexural strength. Also, in terms of the fracture mechanics, it has been known that the slope variation of the stress–strain curve is caused by the crack deflection mechanism; this phenomenon is called the subcritical crack growth [1].

Fig. 10 shows the fracture toughness of monolithic AlN and AlN–W composites. The toughness of composites was increased with increase of the tungsten content. As shown in crack propagation path of Fig. 11, the crack deflection around secondary phase will be caused by grain boundary phases and secondary phase [14]. The compressive stress which increased with the addition of tungsten phase will contribute to the enlargement of crack tortuosity [16], also, the effect of relative density will be included. Thus, crack deflection will minimize the tensile stress concentration around the crack tip in the process of crack propagation. Finally, it was found that the improvement of fracture toughness in AlN–W composites was caused by crack deflection around the secondary phase and grain boundary phases, and by compressive stress distribution.

4. Conclusions

AlN–W composites were densified through pressureless sintering. The grain growth of matrix was gradually inhibited with the addition of tungsten. It was thought that the densification behaviour was caused by the rearrangement and solution–reprecipitation under the presence of liquid phases. These oxide phases at grain boundary were detected in the types of oxides and solid-solution phase by X-ray phase analysis. Fracture strength of composites decreased with the increase of tungsten volume contents. This result seems to be because of the presence of grain boundary phases and the effect of relative density. On the other hand, slope variation around fracture stress value in stress–strain curve was observed, and it was assumed that subcritical crack growth would have occurred by the crack deflection mechanism in the process of crack propagation. The fracture toughness of composites was increased with the addition of tungsten; this would be caused by the restraint of tensile stress concentration by the grain boundary phases and the secondary phase and the residual stress distribution, also, these factors were identified by the observation of microstructure and the X-ray residual stress measurement.

References

1. R. WARREN, "Ceramic–matrix composites" (Blackie and Son Ltd., Glasgow, 1992), p. 4.
2. T. A. MICHALSKE, J. R. HELLMANN, *J. Amer. Ceram. Soc.* **71** (1988) 725.
3. A. ABUHASAN, C. BALASINGH and P. PREDECKI, *ibid.* **73** (1990) 2474.
4. D. J. MAGLEY, R. A. WINHOLTZ and K. T. FABER, *ibid.* **73** (1990) 1641.
5. I. C. NOYAN and J. B. COHEN, "Residual Stress" (Springer-Verlag, New York, 1987) p. 117.
6. V. D. KRSTIC and M. D. VLAJIC, *Acta Metall.* **31** (1983) 139.
7. M. F. YAN, K. NIWA, H. M. O'BRYAN, Jr and W. S. YOUNG, *Adv. Ceram.* **26** (1989) 33.
8. Y. KUROKAWA, C. TOY and W. D. SCOTT, *J. Amer. Ceram. Soc.* **72** (1989) 612.
9. A. ABID, R. BENSALEM and B. J. SEALY, *J. Mater. Sci.* **21** (1986) 1301.
10. R. S. ROTH, J. R. DENNIS and H. F. MCMURIZE, "Phase diagram for ceramists", vol. 2, Fig. 2350, Compiled at the National Bureau of Standard, edited and published by The American Ceramic Society, Inc. (1969).
11. W. D. KINGERY, in "Sintering", key papers, edited by Shigeuki Somiya and Y. Moriyoshi (Elsevier, 1989) p. 383.
12. W. D. KINGERY and M. D. NARASHIMHAN, in "Sintering", key papers, edited by Shigeuki Somiya and Y. Moriyoshi (Elsevier, 1989) p. 395.
13. R. M. GERMAN, "Liquid Phase Sintering" (Plenum, 1985) 65.
14. R. I. TODD and B. DERBY, "Second Euro-Ceramics", Vol. 2, (Augsburg, FRG, 1991), p. 1425.
15. J. MENCIK, "Strength and fracture of glass and ceramics", Glass Science and Technology **12** (Elsevier, Amsterdam New York Tokyo, 1992) p. 56.
16. K. T. FABER, PhD thesis University of California, Berkeley (1982).

Received 28 August 1996
and accepted 12 September 1997